

Modeling the Response of Flexible Risers in the Quasi-steady Regime

擬定常領域におけるフレキシブルライザーの応答モデル

Carlos RIVEROS¹, Tomoaki UTSUNOMIYA², Katsuya MAEDA³ and Kazuaki ITOH⁴

カルロス リベロス, 宇都宮智昭, 前田克弥, 伊藤和彰

¹Student Member of JSCE, M. Eng., Dept. of Civil and Earth Resources Eng., Kyoto University
(Katsura Campus, Nishikyo-ku, Kyoto 615-8540, Japan)

²Member of JSCE, Dr. Eng., Associate Professor, Dept. of Civil and Earth Resources Eng., Kyoto University
(Katsura Campus, Nishikyo-ku, Kyoto 615-8540, Japan)

³Ph.D., Deep Sea Technology Research Group, National Maritime Research Institute
(6-38-1, Shinkawa, Mitaka-shi, Tokyo 181-0004, Japan)

⁴Dr. Eng., Marine Technology Research and Development Program, Marine Technology Center, JAMSTEC
(2-15, Natushima-cho, Yokosuka 237-0061, Japan)

Flexible risers are becoming increasingly important for deep-sea oil production. In addition, current attempts directed towards global warming mitigation target the use of flexible risers for carbon dioxide injection in deep waters. The main difficulties arise from the highly nonlinear behavior and self-regulated nature of flexible risers in marine environments. This paper presents the experimental validation of a response prediction model in the quasi-steady regime. A 20-meter riser model, pinned at its both ends with a constant tension force at its top end, is sinusoidally excited at values of Keulegan-Carpenter Number located in the quasi-steady regime. Good agreement in amplitude response is obtained between experimental data and simulation results.

Key Words: flexible riser, vortex-induced vibration, oscillatory flow, quasi-steady regime.

1. Introduction

The design of flexible pipes “risers” for oil production in deep waters currently considers large safety factors. Therefore, related ongoing research mainly deals with a better understanding of the main factors that influence the response of flexible risers in marine environments. The kinematics of Vortex-Induced Vibration (VIV) is an inherently nonlinear, self-regulated, and multi-degree-of-freedom phenomenon. On the other hand, turbulence remains poorly understood making Computational Fluid Dynamics (CFD)-based approaches restricted for industrial design as reported by Sarpkaya¹⁾. Most of the progress that has been recently achieved in numerical prediction of VIV is mainly restricted to low-Reynolds (Re) number regime. Therefore, considering that practical applications are not located in this regime most of widely used prediction models for flexible risers are semi-empirical and hence based on large databases of hydrodynamic force coefficients experimentally derived.

Sarpkaya¹⁾ highlighted the existing inability to predict the dynamic response of fluid-structure interactions. Among many other factors, the dominant response frequency, the variation of the phase angle and the response amplitude in the synchronization range are still not appropriately understood. Riveros *et al.*²⁾ presented a response prediction model for flexible risers at low values of Keulegan-Carpenter (KC) number. As previously mentioned, CFD usually provides good simulation results in the low-Reynolds number regime. Therefore, Riveros *et al.*²⁾ experimentally validated their proposed response prediction model using CFD-derived force coefficients. However, large discrepancies were found in frequency content in the cross-flow direction and FFT analysis of the experimental data showed that the dominant response frequency does not solely depend on the KC number²⁾. Variation of the phase angle also has large influence on the cross-flow response achieved by an oscillating flexible riser. The dominant response frequency and variation of phase angle still remain in the descriptive realm of knowledge.

Jung *et al.*³⁾ conducted an experimental study using a flexible free hanging pipe in calm water. The pipe was excited in the quasi-steady regime and in-line response was computed using a finite-element based approach and compared with experimental data. Some differences were found for the lower part of the pipe due to large interaction between in-line motion and vortex-induced transverse motion. Vandivier and Jong⁴⁾ proved the existence of a quadratic relationship between in-line motion and cross-flow motion under both lock-in and non-lock-in conditions for VIV of cylinders.

Basically, response prediction of risers is an active research area. So far, the majority of experiments have been conducted in stepped current. One remarkable study was presented by Chaplin *et al.*⁵⁾ that using experimental data and 11 different response prediction models showed that the semi-empirical approach is more successful at predicting the cross-flow response of a flexible riser than the CFD-based approach. On the other hand, risers are usually subjected to a combined loading of waves and currents. The experimental work conducted by Duggal and Niedzwecki⁶⁾ using a 17-meter riser model in oscillatory flow proved that the cross-flow response show similarities with previous research work using oscillatory flow in rigid cylinders. Finally, the experimental work presented by Park *et al.*⁷⁾ using a 6-meter riser model showed that good agreement between experiments and numerical simulation is only possible if enhanced drag coefficients due to VIV are included. The above-mentioned facts show the importance of correctly relate both in-line and cross-flow motions in the development of any prediction model for risers.

This paper presents the experimental validation of the response prediction model for flexible risers previously developed by Riveros *et al.*²⁾. The experimental validation is carried out in the quasi-steady regime ($KC > 30$). At low values of KC number inertial forces are dominant. On the other hand, in the quasi-steady regime drag forces control the response of a flexible riser. In this paper, the previously developed prediction model is extended to large values of KC number. The response prediction model considers increased mean drag coefficients during synchronization events and amplitude dependent lift coefficients.

2. Response Prediction Model

A Cartesian reference is defined in the x -axis by the force motion at the top end of the riser, the z -axis is defined in the direction of the riser's axis and the y -axis is perpendicular to both as shown in Fig.1.

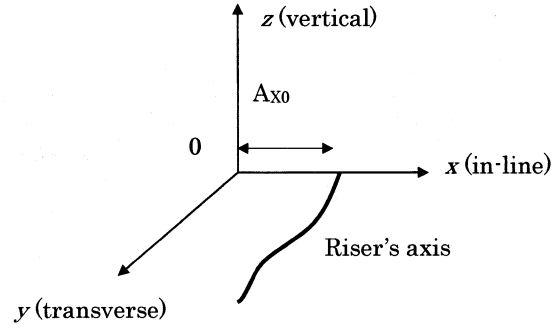


Fig.1 Riser Motion and Coordinate System.

The response prediction model previously presented by Riveros *et al.*²⁾ is used in this paper. The riser is therefore idealized as a beam with low flexural stiffness using the Euler-Bernoulli beam equation as shown in Eq. (1).

$$EI \frac{\partial^4 u_{x,y}(z,t)}{\partial z^4} - \frac{\partial}{\partial z} \left[(T_i - w(L-z)) \frac{\partial u_{x,y}(z,t)}{\partial z} \right] + c_0 \frac{\partial u_{x,y}(z,t)}{\partial t} + m_0 \frac{\partial^2 u_{x,y}(z,t)}{\partial t^2} = F_{T_{x,y}}(z,t) \quad (1)$$

where m_0 is the mass of the riser per unit length, $u_{x,y}(z,t)$ is the deflection, c_0 is the damping coefficient, EI is the flexural stiffness, T_i is the tension applied at the top of the riser, L is the length of the riser and w is the submerged weight. The external fluid force is $F_{T_{x,y}}$. The in-line force acting on a riser is represented according to the formulation presented by Carberry *et al.*⁸⁾ as shown in Eq. (2)

$$F_{T_x}(z,t) = \rho S C_m \dot{U}_1 - \rho S C_i \ddot{u}_x + \frac{1}{2} \rho D (U_1 - \dot{u}_x) |U_1 - \dot{u}_x| \left[C_{Dmean} + C_D \sin(2(2\pi f_L + \phi_{drag})) \right] \quad (2)$$

where ρ is the density of the surrounding fluid, S is the cross-sectional area of the displaced fluid, U_1 is the steady velocity of the fluid in the in-line direction and D is the diameter of the riser. The mean drag coefficient is denoted by C_{Dmean} , the fluctuating drag coefficient by C_D , the inertia coefficient by C_m and the added-mass coefficient by C_i . f_L is the dominant frequency defined as the most dominant frequency in the y -axis or cross-flow direction. ϕ_{drag} is the phase of the drag with respect to the cylinder's displacement in the cross-flow direction. The dominant frequency is related to the cross-flow motion and is used to calculate the

transverse force as shown in Eq. (3).

$$F_{T_y}(z,t) = \frac{1}{2} \rho D U_0^2 C_L \sin(2\pi t f_L + \phi_{lft} + \Delta\theta(z)) \quad (3)$$

Here, U_0 is the relative in-line maximum velocity. C_L is the lift coefficient and ϕ_{lft} is the phase with respect to the cross-flow displacement. $\Delta\theta(z)$ is related to an initial phase angle that is used to couple in-line and cross-flow motions allowing the correct application of $F_{T_y}(z,t)$ for a particular section of the riser and considering the existing difference in the values of phase angle of the traveling wave originated at the top end of the riser and the remaining regions in the case of a riser excited at its top end, which is the case considered in this paper. Detailed explanation related to the numerical calculation of this parameter is provided in Section 4. C_L varies with the amplitude of the cross-flow motion (A_y) according to the empirical formulation presented by Blevins⁹⁾, which is shown in Eq. (4).

$$C_L = 0.35 + 0.6 \left(\frac{A_y}{D} \right) - 0.93 \left(\frac{A_y}{D} \right)^2 \quad (4)$$

Sarpkaya¹⁾ defined synchronization as a phase transformer due to the fact that synchronization produces a rapid inertial force decrement and a rapid increment of the absolute value of the drag force. According to Pantazopoulos¹⁰⁾, in the lock-in or synchronization region, lift, added mass, and damping forces cannot be distinguished, and only amplitude and phase of the total hydrodynamic force can be determined. At frequencies far above the synchronization region, added mass is equal to its nominal value of unity. At frequencies above the synchronization region, added mass increases near 2.0, which is similar to the case of oscillatory flow past a stationary cylinder. At frequencies below the synchronization region, the cross-flow added mass coefficient becomes negative. This variation tends to change the natural frequency of the cylinder toward the synchronization region. As a result, the cross-flow added mass coefficient is generally frequency-dependent, but relatively insensitive to amplitude and there is a tendency for the negative added mass values to increase as the cross-flow amplitude A_y increases.

The damping coefficient is strongly dependent on A_y and somewhat less sensitive to frequency outside the synchronization region. This dependence is much stronger at frequencies above the

synchronization region than frequencies below the synchronization region. At frequencies above and below the synchronization region, the damping coefficient is consistent with typical drag coefficient data. Within the synchronization region, it is not possible to separate damping from lift as previously mentioned and therefore the resulting force term proportional to cylinder velocity is frequency and amplitude dependent¹⁰⁾.

Khalak and Williamson¹¹⁾ reported an increase of 3.5 times in the mean drag coefficient of an oscillating cylinder involving simultaneous oscillations in the in-line and the cross-flow directions when is compared with the case of static cylinder. The increased mean drag coefficient (C_{Dinc}) model employed in this paper corresponds to an empirical formulation presented by Khalak and Williamson¹¹⁾, which is shown in Eq. (5).

$$\frac{C_{Dinc}}{C_{Dmean}} = 1.0 + 2.0 \left(\frac{A_y}{D} \right) \quad (5)$$

Sarpkaya¹²⁾ made a clear distinction between vortex-shedding excitation and hydrodynamic damping. The latter is associated to an oscillating body in a fluid otherwise at rest and implies a decrease of the amplitude of the externally imparted oscillation by forces in anti-phase with velocity. It is clear that the un-separated flow about the oscillating body does not give rise to oscillatory forces in any direction and, thus, it cannot excite the body. Sarpkaya¹²⁾ highlighted that hydrodynamic damping is still used to lump into one parameter the existing inability to predict the dynamic response of fluid-structure interactions.

3. Experimental Model

Large-scale experiments are conducted to validate the proposed prediction model. The experimental validation is carried out in the Integrated Laboratory for Marine Environmental Protection (National Maritime Research Institute). **Fig.2** depicts the deep-sea basin, which consists of a circular basin (depth: 5m, effective diameter: 14m) and a deep pit (depth: 30m, effective diameter: 6m). The 3-dimensional measurement equipment is composed of 20 high-resolution digital cameras.

A 20-meter riser model is used to validate the response prediction model in the quasi-steady regime. Forced harmonic motion with amplitude of 0.08 m and period of 2 seconds is selected based on the value of KC number presented by Jung *et al.*³⁾. Therefore, experimental validation of the prediction model is carried out in the quasi-steady regime.

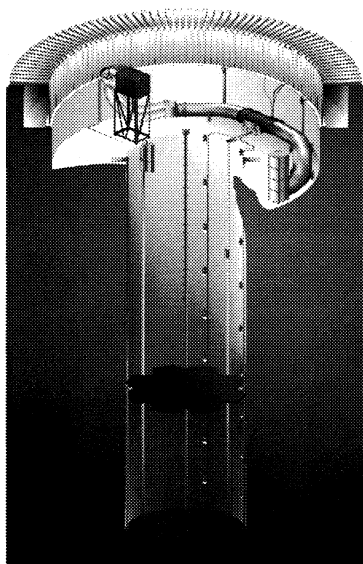


Fig.2 Deep-Sea Basin (NMRI).

Table 1 Properties of the Riser Model.

Material	Polyoxymethylene
Model length (m)	20
Outer diameter D (m)	0.0160
Inner diameter (m)	0.0108
Density (kg/m ³)	1410
Young's modulus (MPa)	2.937

The model is excited in still water and steel bars are added to the riser model in order to increase its self-weight. The total weight of the riser, including the steel bars, is 68.14 N. Pinned connections are used at its both ends and the tension force, applied at its top end, corresponds to 63.5 N. The properties of the experimental model are presented in Table 1.

4. Numerical Implementation

The commercial software ABAQUS¹³⁾ is used to solve Eq. (1). The numerical model of the riser is composed of 40 cubic pipe elements. A nonlinear time-domain method is selected in order to apply the riser's self-weight and therefore geometric nonlinearity is considered. The direct-integration method is used to compute the dynamic response of the riser. A FORTRAN subroutine developed by Riveros *et al.*²⁾ calculates displacements, velocities and accelerations at each time step in order to numerically implement the amplitude-dependent lift and increased mean drag coefficient models. Inertia and drag coefficients experimentally computed by Obasaju *et al.*¹⁴⁾ at $\beta = 196$ are used for the numerical implementation of the proposed prediction model. ($\beta = Re/KC$). The simulation results presented by Lin *et al.*¹⁵⁾ are used for $KC < 4$.

The magnitude of KC indicates different flow modes. Several authors have described the flow regimes observed in oscillatory flow past a stationary cylinder. Among many others descriptions, the ones provided by Bearman *et al.*¹⁶⁾ and Williamson¹⁷⁾ are cited most frequently. According to Lin *et al.*¹⁵⁾, at low values of KC , $1 < KC < 2$, depending on β , the flow is symmetrical and remains attached to the cylinder. At $KC \approx 4$, the flow separates but remains symmetrical as concentrations of vorticity are swept back over the cylinder when the flow reverses. Then, the asymmetric shedding of a pair of opposite sign vortices is observed in each half cycle for $4 < KC < 7$. Obasaju *et al.*¹⁴⁾ stated that above $KC = 7$ a new regime is achieved as KC is increased in increments of about 8 leading to one more full vortex to be shed per half cycle of flow oscillation. At $7 < KC < 15$ most of the vortex shedding activity is concentrated on one side of the cylinder. Lin *et al.*¹⁵⁾ experimentally stated that "around $KC = 10$ the transverse force is approximately at twice the flow frequency but now and then an extra vortex appears to be generated". At $15 < KC < 24$ the flow enters the diagonal shedding mode consisting of a pair of oppositely signed vortices that convects away at about 45° to the main flow in one half cycle and another pair of vortices that convects in a diametrically opposite direction in the next half cycle. At $24 < KC < 32$ three full vortices are shed during each half cycle and three vortex pairs convect away from the cylinder for a complete cycle. This trend is maintained as KC increases with more and more vortex pairs being formed and shed per flow cycle. Fig.3 shows the values of C_{Dmean} and Fig.4 the values of $C_i = C_m - 1.0$.

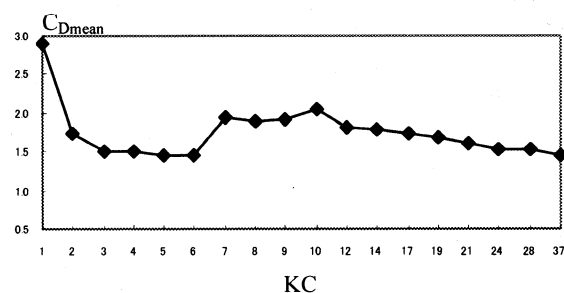


Fig.3 C_{Dmean} (Lin *et al.*¹⁰⁾; Obasaju *et al.*⁹⁾).

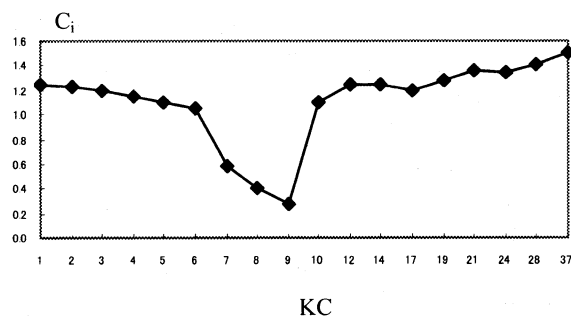


Fig.4 C_i (Lin *et al.*¹⁰⁾; Obasaju *et al.*⁹⁾).

It is important to note that Lin *et al.*¹⁵⁾ identified the existence of a region located around $KC=10$ where there is a rapid rise of C_{Dmean} and decrease of C_M . The mean drag coefficient rises approximately from 1.5 at $KC=6$ to 2.1 at $KC=10$. According to Lin *et al.*¹⁵⁾, two-dimensional simulation around $KC=10$ fails to predict this peak due to three-dimensional flow features. On the other hand, there is a rapid decrease of C_M in the same region ($6 < KC < 10$). It was experimentally proved that there is a range of β in which C_{Dmean} is not sensitive to changing β . Its upper boundary lies between $\beta=964$ and 1204 ¹⁴⁾. The value of the beta parameter achieved by the riser model is 128. Therefore, it is not expected large variation in the hydrodynamic coefficients employed in this paper. According to Blevins⁹⁾, in-line VIV usually occurs with twice of the shedding frequency in the range $2.7 < U_r < 3.8$. Where $U_r = U_l / (f_{osc} D)$ and f_{osc} is the oscillating frequency of the body. The FORTRAN subroutine computes U_r at each time step and compares its value with the aforementioned limits in order to include the fluctuating drag force part of Eq. (2). On the other hand, synchronization events in the cross-flow direction are considered to occur if $4 < U_r < 8$ ¹⁾ leading to increased drag force based on Eq. (5). $\phi_{lift}=0$, $\phi_{drag}=0$ and $C_D=0.2$ are selected based on the experimental work presented by Carberry *et al.*⁸⁾. Finally, a structural damping ratio of 0.3% is included in the prediction model based on the experiments conducted by Huera-Huarte *et al.*¹⁸⁾.

The numerical implementation of the proposed prediction model is carried out in three stages. The main consideration is that hydrodynamic force coefficients need to be updated based on the values of the KC numbers achieved by each of the sections in which the riser is divided. The first stage consists of 25 cycles and uses hydrodynamic forces with fixed coefficients values. Then, at the end of the first stage, in-line amplitudes are computed in order to calculate the KC values for each section of the riser and update drag coefficients. In the second stage, cross-flow forces are applied during 10 additional cycles. Synchronization events are considered in the third stage after updating hydrodynamic force coefficients. f_L is a function of KC and S_r , which are herein computed based on the empirical formulation derived by Norberg¹⁹⁾.

The numerical implementation of Eq. (3) requires the correct calculation of $\Delta\theta(z)$. However, the initial riser's response is transient due to a time-varying load. It takes approximately 4 seconds for the wave originated at the top end of the riser to completely excite its bottom end. Then, the steady response is achieved and all sections of the model

are excited at different frequencies, amplitudes and phase angles. Therefore, an algorithm is used to approximately compute $\Delta\theta(z)$ by using the difference between the time required for each section of the model to achieve its maximum in-line displacement and the time at the top end of the riser to achieve the same condition. Therefore, $\Delta\theta(z)$ allows the correct application of $F_{T_v}(z,t)$ at the end of the first stage. The main consideration behind the use of this parameter is that it considers the existing differences in the in-line phase angles for all the sections in which the riser is divided. As a result, $F_{T_v}(z,t)$ is correctly applied at the beginning of the second stage. Otherwise, wrong in-line amplitudes obtained during the transient response may under-estimate the phase angle and lead to out-of-phase response between the in-line and the cross-flow motions of the riser.

5. Simulation Results

As previously mentioned, a former validation of the response prediction model was conducted by Riveros *et al.*²⁾ at low values of KC number ($KC < 4$). It is important to note that it is widely accepted the calculation of the dominant frequency as a direct function of the KC number. Blevins⁹⁾ provides a table in which the values of the dominant frequency for each of the regimes proposed by Obasaju *et al.*¹⁴⁾ are given. In the quasi-steady regime drag forces are dominant over inertial forces. Also there is an increment of the magnitude of the transverse forces as shown in Eq. (3). The main objective of the study in this paper is to experimentally validate the prediction model developed by Riveros *et al.*²⁾ in the quasi-steady regime. The experimental data were passed through a 6th order high-pass Butterworth filter with a 0.1 Hz cutoff. The in-line phase angles were corrected in order to improve the quality of the graphical results. Variations in the phase angles were found when the experimental results were compared with simulation results. These variations may be caused in part by the initial unsteady response of the riser. In-line and cross-flow responses are computed at depths of 3.5 m, 6.5 m, 9 m, 12 m, 14.5 m and 17 m. **Figs. 5, 6 and 7** show the time history response of the riser during 14 seconds. In-line response in both amplitude and frequency content is well predicted. The response prediction model correctly accounts for drag force amplification during synchronization events. On the other hand, although experimental data show some non-linearities in the in-line response, the simulation results follow the main trend of the riser's response.

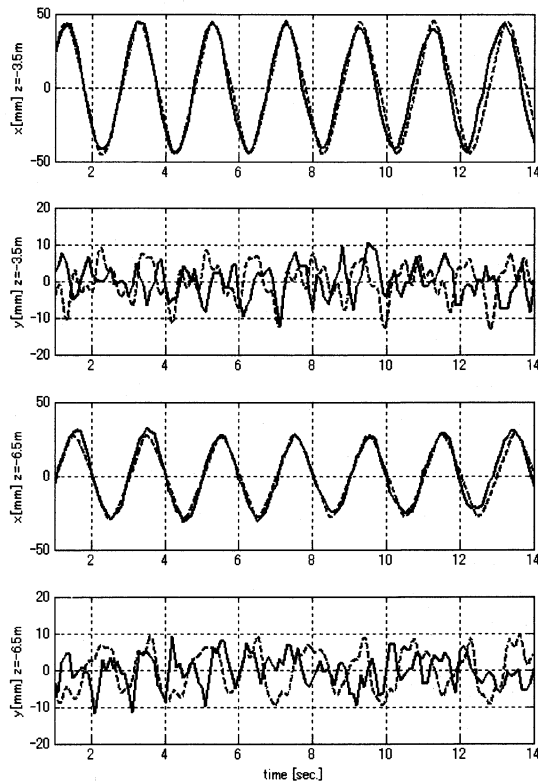


Fig.5 Time History Response at $z=-3.5\text{m}$ and $z=-6.5\text{m}$
 ---- Simulation — Experiment

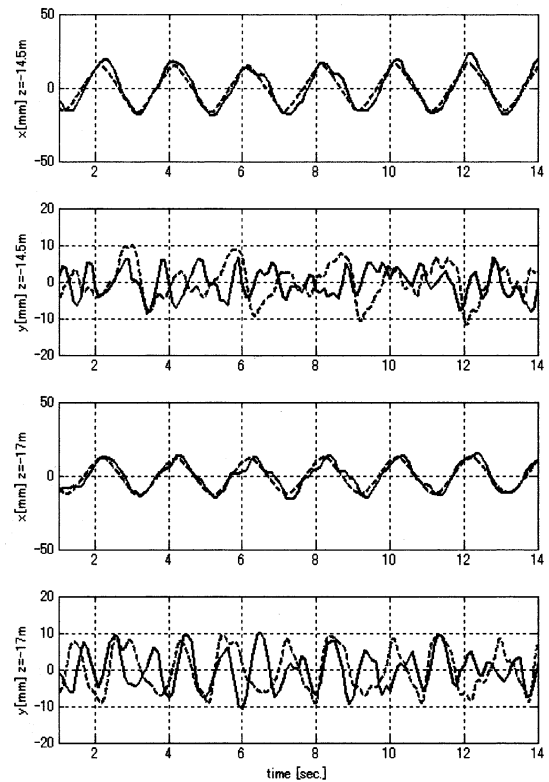


Fig.7 Time History Response at $z=-14.5\text{m}$ and $z=-17\text{m}$
 ---- Simulation — Experiment

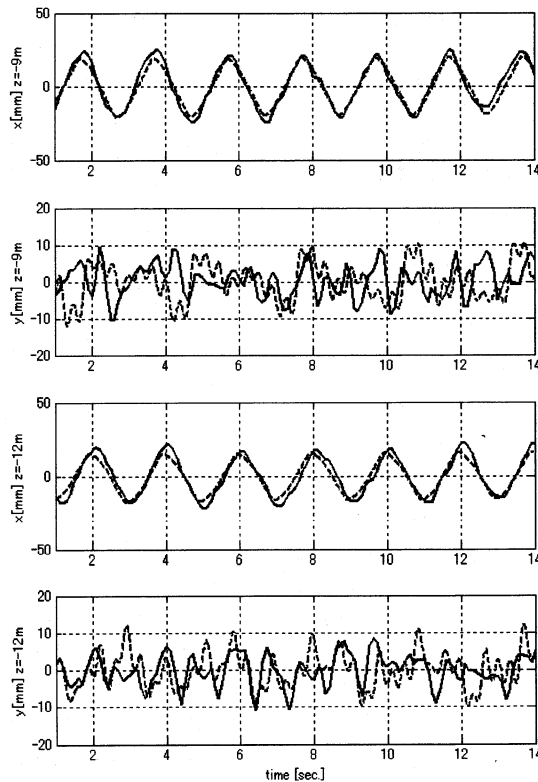


Fig.6 Time History Response at $z=-9\text{m}$ and $z=-12\text{m}$
 ---- Simulation — Experiment

Cross-flow response is also relatively well predicted for the cases presented in **Figs. 5, 6 and 7**. It can be observed that the sinusoidal approximation widely used to describe the cross-flow response based on the dominant frequency is not applicable for practical applications. Even though transverse force is calculated based on Eq. (3), the experimental data show large fluid-structure interaction leading to non-sinusoidal cross flow response as shown in **Figs. 5, 6 and 7**. As previously mentioned, the initial riser's response is unsteady due to time varying load. Therefore, when comparisons between experimental data and simulation results were conducted, it was necessary to modify in-line phase angles in order to improve the quality of the graphical results presented in **Figs. 5, 6 and 7**. Variations in the phase angles in both in-line and cross-flow response were found when the experimental results were compared with simulation results. These variations may be caused in part by the initial unsteady response.

According to Blevins⁹⁾, the dominant frequency in the quasi-steady regime can be approximately calculated as 6 times the value of its corresponding in-line frequency. However, the experimental data show high variation in both amplitude and frequency content in the cross-flow response. Based on the aforementioned, the response prediction

model accounts for the main features of the riser response and achieves good agreement in both amplitude and frequency content. This is basically a current limitation in the theory related to main factors that influence the response of oscillating flexible risers. Another important factor to be considered is the mass-damping parameter ($m^*\zeta$), where m^* is the mass ratio calculated as the mass of a body divided by the mass of the fluid displaced and ζ is defined as the ratio of ((structural damping)/(critical damping)). Based on the work presented by Willdem and Graham²⁰, at low values of mass ratio ($m^* < 3.3$), the fluid is dominant over the structure leading to a joint response dominated by the fluid and therefore their joint response frequency will be controlled by the Strouhal frequency. The importance of m^* is mainly related to the existing link between m^* and C_m . According to Sarpkaya¹, C_m becomes increasingly important as the m^* becomes smaller. Therefore, it is expected improvement in response prediction in the quasi-steady regime, because this regime is mainly dominated by drag forces. Sarpkaya¹² decomposed the instantaneous cross-flow force using a two-coefficient model into inertia and drag components in order to study its dependency on the cross-flow amplitude. Three representative values of A_y/D ($=0.25, 0.50$ and 0.75) were used to experimentally prove that the drag component of the instantaneous cross-flow force becomes negative in the vicinity of the synchronization region defined as the matching of the shedding frequency and the natural frequency of the cylinder in the cross-flow direction. This negative component of the drag force is commonly defined as negative damping and therefore produces amplification of the oscillations. Sarpkaya¹² proved that the maximum negative amplitude of the drag component of the cross-flow force is achieved around $A_y/D=0.5$ and then decreases. The oscillations become self-limiting for A_y/D larger than about unity. As noted by Sarpkaya¹, the larger the amplitude of VIV oscillations, the more nonlinear is the dependence of the lift forces on A_y/D . Considering the aforementioned facts, it is possible to infer that accurate prediction of the cross-flow response when $A_y/D > 0.5$ is still not feasible. It is also possible to observe in Figs. 5, 6 and 7 that the maximum amplitude of the cross-flow motion overpasses the aforementioned limit. The peaks are located around 0.01 m. Amplitude of the cross-flow motion plays a crucial role as previously mentioned. However, the correct prediction of the frequency content of the cross-flow motion is even more challenging. There are basically two main limitations; the first one is related to the existence of synchronization events.

As a result, outside synchronization regions the force experienced by the riser will contain both the Strouhal and body oscillations¹. On the other hand, synchronization causes the matching of the vortex shedding and oscillation frequencies leading to "an increase in the spanwise correlation of the vortex shedding and a substantial amplification of the cylinder's vibrational response"²⁰. The second limitation is related to ϕ_{liff} . According to Morse and Williamson²¹, ϕ_{liff} is crucial in determining the energy transfer from the fluid to the riser. At low values of m^* the energy dissipated is low and a small variation of ϕ_{liff} can induce the system to change from positive to negative excitation.

Finally, FFT amplitudes are computed for all the sections of the riser in both in-line and cross-flow directions and depicted in Figs. 8 and 9, respectively.

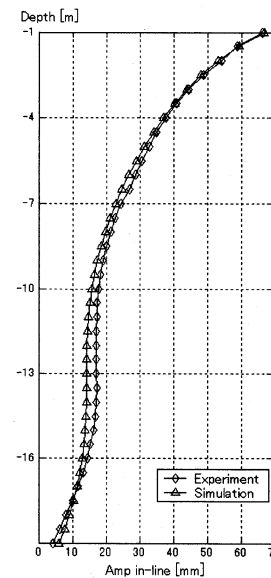


Fig.8 FFT Amplitudes
In-line Direction

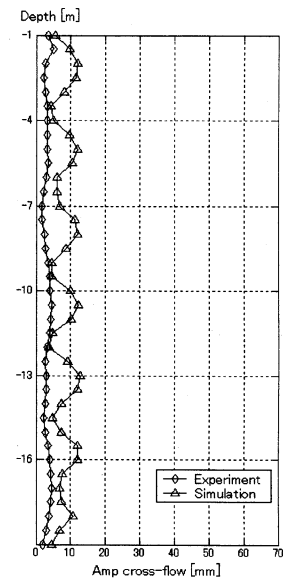


Fig.9 FFT Amplitudes
Cross-Flow Direction

It is possible to observe significant differences in the cross-flow direction due to the non-sinusoidal response of the riser. It is widely recognized that the cross-flow response of flexible risers is an inherently nonlinear, self-regulated and multi-dof phenomenon. The main concern is that existing models for cross-flow response of risers are based on a single frequency component. This is actually a current limitation. As previously mentioned, Riveros *et al.*² based FFT analysis of experimental data showed that it is not correct the assumption that the dominant response frequency only depends on the KC number. Therefore the use of FFT amplitudes in the cross-flow direction does not consider the contribution of other relevant frequencies and their corresponding amplitudes.

6. Conclusions

In this paper, the experimental validation of a previously developed response prediction model for oscillating flexible risers was presented. This validation was conducted in the quasi-steady regime, where drag forces are dominant over inertial forces. A 20-meter riser model was selected based on the experimental work conducted by Jung *et al.*³⁾. The response prediction model considers amplitude-dependent lift coefficients and an increased drag coefficient model in order to take into account drag amplification during synchronization events. In-line response was well predicted in both amplitude and frequency content. Cross-flow displacements were also well predicted considering the nonlinear nature of the VIV process. It is important to note that in this paper it is assumed amplitude-dependent lift coefficients. Therefore, cross-flow response is more accurately predicted when $A_y/D < 0.5$. As previously mentioned, VIV oscillations become more nonlinear when $A_y/D > 0.5$. Most of the cross-flow displacements achieved by the experimental model presented in this paper are located beyond the aforementioned limit. The accurate prediction of the cross-flow response in flexible risers is still challenging due to its highly nonlinear nature. In addition, the assumption that only one frequency dominates the cross-flow response may introduce considerable deviations in its numerical calculation. The simulation results presented in this paper agree well with previous findings. The response prediction of an oscillating flexible riser involves several challenges due to the nonlinear and self-regulated nature of the VIV process. It has been sufficiently proved that synchronization events cause an increase of cross-flow displacements leading to a sudden increase in the drag force and therefore affect the whole in-line response of the riser. Furthermore, the dynamic response of a flexible riser having a value of mass ratio lower than 3.3 is more complex due to the existence of 3 modes of response in contrast with the 2 modes of response found in risers having values of mass ratio larger than 10. Considering current limitations in predicting the dynamic response of flexible risers, this paper presents a practical methodology for response prediction of oscillating flexible risers.

REFERENCES

- 1) Sarpkaya, T. : A critical review of the intrinsic nature of vortex-induced vibrations, *Journal of Fluids and Structures*, Vol. 19, pp. 389-447, 2004.
- 2) Riveros, C., Utsunomiya, T., Maeda, K. and Itoh, K. : CFD Modeling of fluid-structure interaction for oscillating flexible risers, *Journal of Applied Mechanics JSCE*, Vol. 10, pp. 1099-1108, 2007.
- 3) Jung, D.H., Park, H.I., Koterayama, W. and Kim, H.J. : Vibration of highly flexible free hanging pipe in calm water, *Ocean Engineering*, Vol. 32, pp. 1726-1739, 2005.
- 4) Vandivier, J.K. and Jong, Y.J. : The relationship between in-line and cross-flow vortex-induced vibration of cylinders, *Journal of Fluids and Structures*, Vol. 1, pp. 381-399, 1987.
- 5) Chaplin, J.R., Bearman, P.W., Cheng, Y., Fontaine, E., Graham, J.M.R., Herfjord, M., Isherwood, M., Lambrakos, K., Larsen, C.M., Meneghini, J.R., Moe, G., Triantafyllou, M.S. and Willden, R.H.J. : Blind predictions of laboratory measurements of vortex-induced vibrations of a tension riser, *Journal of Fluids and Structures*, Vol. 21, pp. 25-40, 2005.
- 6) Duggal, A.S. and Niedzwecki, J.M. : Dynamic response of a single flexible cylinder in waves, *ASME Journal of Offshore Mechanics and Arctic Engineering*, Vol. 117, pp. 99-104, 1995.
- 7) Park, H.I., Jung, D.H. and Koterayama, W. : A numerical and experimental study on dynamics of a towed low tension cable, *Applied Ocean Research*, Vol. 25, pp. 289-299, 2003.
- 8) Carberry, J., Sheridan, J. and Rockwell, D. : Controlled oscillations of cylinders: forces and wake modes, *Journal of Fluid Mechanics*, Vol. 538, pp. 31-69, 2005.
- 9) Blevins, R.D. : *Flow-Induced Vibration*, Second Edition, Krieger Publishing Co., Florida, 1990.
- 10) Pantazopoulos, M. S. : Vortex-induced vibration parameters: critical review, *Offshore Technology ASME OMAE*, Vol. 1, pp. 199-255, 1994.
- 11) Khalak, A. and Williamson, C.H.K. : Motions, forces and mode transitions in vortex-induced vibrations at low mass-damping, *Journal of Fluids and Structures*, Vol. 13, pp. 813-851, 1999.
- 12) Sarpkaya, T. : Hydrodynamic damping, flow-induced oscillations, and biharmonic response, *ASME Journal of Offshore Mechanics and Arctic Engineering*, Vol. 117, pp. 232-238, 1995.
- 13) ABAQUS, Standard User's Manual, Version 6.7.
- 14) Obasaju, E.D., Bearman, P.W. and Graham, J.M.R. : A study of forces, circulation and vortex patterns around a circular cylinder in oscillating flow, *Journal of Fluid Mechanics*, Vol. 196, pp. 467-494, 1988.
- 15) Lin, X.W., Bearman, P.W. and Graham, J.M.R. : A numerical study of oscillatory flow about a circular cylinder for low values of beta parameter, *Journal of Fluids and Structures*, Vol. 10, pp. 501-526, 1996.
- 16) Bearman, P.W., Downie, M., Graham, J.M.R. and Obasaju, E.D. : Forces on cylinders in viscous oscillatory flow at low Keulegan-Carpenter number, *Journal of Fluid Mechanics*, Vol. 154, pp. 337-356, 1985.
- 17) Williamson, C.H.K. : Sinusoidal flow relative to circular cylinders, *Journal of Fluid Mechanics*, Vol. 155, pp. 141-174, 1985.
- 18) Huera-Huarte, F.J., Bearman, P.W. and Chaplin J.R. : On the force distribution along the axis of a flexible circular cylinder undergoing multi-mode vortex-induced vibrations, *Journal of Fluids and Structures*, Vol. 22, pp. 897-903, 2006.
- 19) Norberg, C. : Fluctuating lift on a circular cylinder: review and new measurements, *Journal of Fluids and Structures*, Vol. 17, pp. 57-96, 2003.
- 20) Willden, R.H.J. and Graham, J.M.R. : Three-distinct response regimes for the transverse vortex-induced vibrations of circular cylinders at low Reynolds numbers, *Journal of Fluids and Structures*, Vol. 22, pp. 885-895, 2006.
- 21) Morse, T.L. and Williamson, C.H.K. : Employed controlled vibrations to predict fluid forces on a cylinder undergoing vortex-induced vibration, *Journal of Fluids and Structures*, Vol. 22, pp. 877-884, 2006.

(Received April 14, 2008)